ESTIMATION OF FRACTURE PARAMETERS AFTER REMOVING ANISOTROPIC OVERBURDEN EFFECT

Mohammed Alhussain and Mrinal K. Sen

Department of Geological Sciences
The University of Texas at Austin

ABSTRACT

Estimation of reservoir fracture parameters such as fracture orientation and density or fracture normal and tangential weakness (ΔN and ΔT respectively) from seismic data is often difficult because of one important question: Is the anisotropy caused by the reservoir interval alone or by the effect of the lithlogic unit above the reservoir? Often hydrocarbon reservoirs represent a small portion of the seismic section and inversion of reservoir anisotropic parameters can be easily obscured by the presence of anisotropic overburden. In this paper, we show examples where we can clearly observe imprints of overburden anisotropic layers on the seismic response of the target zone. Then we present a simple method to remove the effect of anisotropic overburden to recover reservoir fracture parameters. It involves analyzing amplitude variation with offset and azimuth (AVOA) for the top of reservoir reflection amplitude and for a reflector below the reservoir. Seismic gathers are transformed to delay-time slowness (tau-p) domain. We then calculate the ration of the amplitudes picked at the reservoir top and for the reflector beneath the reservoir. The ratio is then used to remove the transmission effect of the overburden. The methodology is applied to two sets of models - one containing a fractured reservoir with isotropic overburden and the other containing a fractured reservoir with anisotropic overburden. Conventional analysis in the x-t domain indicates that the anisotropic overburden has completely obscured the anisotropic signature of the reservoir zone. When the new methodology is applied, the overburden effect is significantly reduced. Inversion of fracture parameters is applied to both conventional AVOA curves and on the new amplitude ratio attribute. We show that the fracture parameter ΔN is estimated accurately whereas ΔT parameter is not stable and could not be recovered using only P-P reflection seismic data.

INTRODUCTION

Cumulative effects of seismic waves propagating in the overburden can distort the amplitudes of seismic reflection from a target reservoir. Hence, erroneous amplitude analysis of the reservoir may result if overburden effects are ignored. Many factors can cause distortion in

amplitudes including regional and local structural variations, sinkholes, shallow channels, and anisotropy in shallow layers. The need to account for such effects has been recognized by Luo et al. (2005, 2007), Liu et al. (2011), and others. Transmission effects caused by the presence of anisotropic layers in the overburden, for example, can easily hinder the AVOA analysis, which can lead to unreliable estimates of anisotropic reservoir parameters (Sen et al., 2007).

For a single set of vertical fractures, the medium can be considered a transversely isotropic medium with a horizontal axis of symmetry or an HTI medium in the low frequency limit (Schoenberg and Douma, 1988, Tsvankin, 2005). Conventional AVOA analysis is mostly done on the reservoir top where vertical fractures cause variation of reflected amplitude with source-receiver offset and azimuth. The AVOA signature from the base of the fractured unit, however, is generally stronger than that from the top. Azimuthal variations from the top of the reservoir depend only on the variation in reflection coefficient, whereas the raypath is also a function of azimuth for reflections from the base of the fractured unit, leading to stronger, more visible variation of AVO with azimuth. This also leads to the conclusion that an azimuthal variation in AVO due to fractures in the overburden may be misinterpreted to be due to the presence of aligned fractures within the reservoir (Sayers and Rickett, 1997).

Two fundamental problems arise when analyzing AVOA of a reservoir bottom pick. The first one is that many petroleum reservoirs are not thick enough to separate top and bottom reflectors given the frequency range of seismic data. Thin bed interference effects (e.g, internal multiples, tuning) would make it difficult to effectively invert for reservoir parameters (Sen et al., 2007). The second problem is that the reservoir bottom reflection is not detected in surface seismic data due to the gradual change from reservoir properties to the layer below reservoir. Analysis of real data used in my study area indicated that second problem is indeed present.

In the first part of this paper, we propose a new technique to remove the effect of transmission from the overburden through picked amplitudes from the reservoir top and from a reflector below the reservoir. In the second part, we quantitatively analyze reservoir fracture properties namely, ΔN and ΔT. We invert both conventional AVOA and the new ratio attribute data, and compare results.

PARAMETER ESTIMATION AND FORWARD MODELING

Estimation of fracture parameters (e.g., number of dominant fracture sets, fracture density and fracture fillings) used as an input to a forward model is based on well logs including Formation MicroImaging (FMI) logs. Despite the fact that FMI logs are not representative of the entire reservoir and are not as popular as conventional well logs, they are a direct measurement and should be weighed heavily in estimating the parameters of our fracture model. A rose

diagram for all open fractures from all horizontal wells for a carbonate oil field in the Arabian Peninsula shows that here we have only one set of vertical fractures oriented approximately ESE-WNW (Figure 1a). Figure 1b shows a histogram of fracture spacing for open fractures for one of the horizontal wells derived from FMI log. The Dominant fracture spacing is 20 cm. The information taken from conventional well logs and FMI logs indicate that the reservoir is porous and fractured; and therefore, we feel that porous fractured forward models would best describe the reservoir. Five independent effective medium parameters are derived for a saturated porous fractured reservoir using the Gurevich (2003) model (Appendix A and B). This model is used here because it uses a reasonable number of parameters to describe porous fractured rocks and is a reasonably good representation of our field.

(a)   (b)
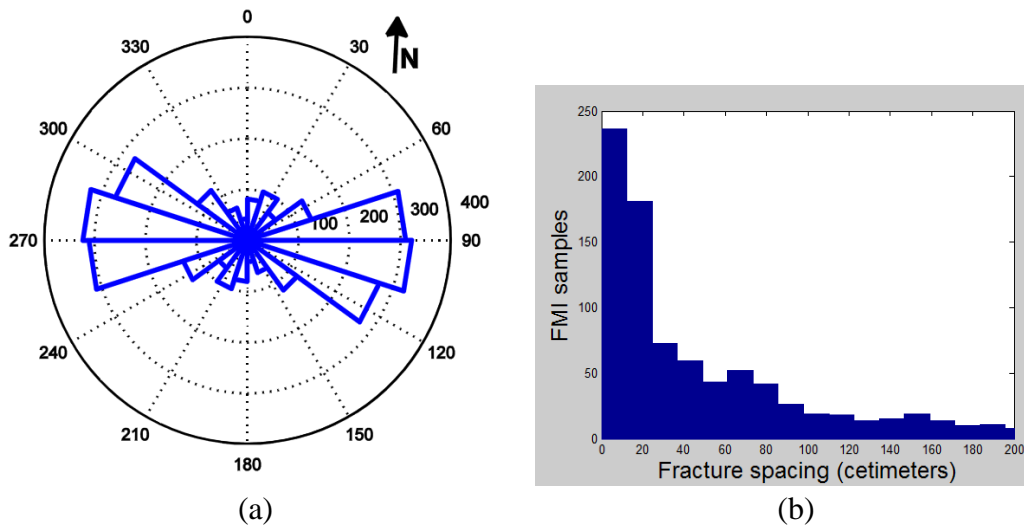
Figure 1. (a) Rose diagram showing fractures dominant azimuthal direction for all wells. The outer circle numbers indicate azimuth and the inner circles indicate number of fractures. (b) Histogram of fracture spacing for open fractures for one of the horizontal wells derived from FMI logs. The Dominant fracture spacing is 20 cm.

Well logs show that the reservoir has a coarsening upward sequence where the quality of the reservoir is gradually improving upward. This is clearly indicated by slower Vp and Vs velocities and lower density values at the top of the reservoir. In order to depict reservoir parameters closely, the reservoir is divided into 14 compartments each with different Vp, Vs, density and prorosity values. Figure 2 shows how these four parameters gradually vary across different depths of the reservoir in a simillar manner to the logs. Crack density is set to be constant in all layers.
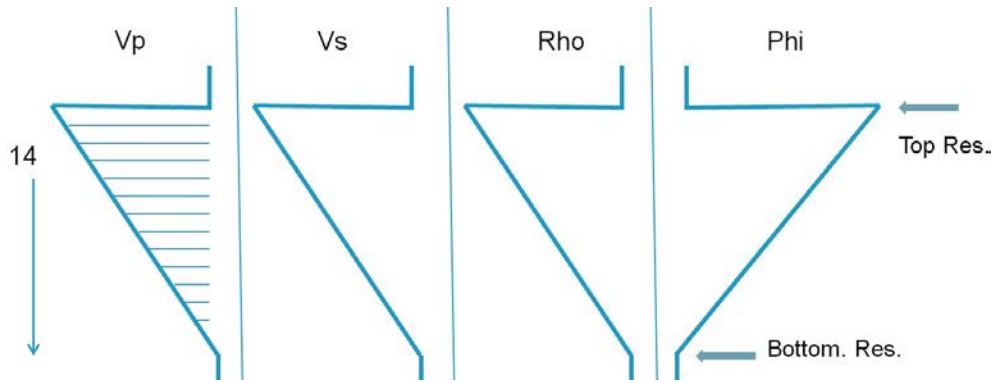
Figure 2. Reservoir interval is divided into 14 different layers. Each layer has a different set of reservoir property values.

In order to investigate the effect of anisotropic overburden on AVOA analysis, two models are considered. The first one consists of an anhydrite cap rock and vertically fractured carbonate reservoir (14 layers as mentioned above) and an isotropic overburden. The second model is the same but with added anisotropic section in the overburden that includes a layer with vertical fractures. Both models can be seen in figure 3 (a, b). Fracture sets in the overburden and in the reservoir are taken to be 90 degrees azimuth relative to each other. Full-waveform numerical simulation is performed on both models for several source-receiver offsets and azimuths (Mallick and Frazer 1991). Offset range from zero to 3200 m in increments of 80 m. The dominant frequency of the wavelet used is 35 Hz and target horizon is at a depth of 1500 m. The resulting gathers, one azimuth for each model, are shown in figure 4.
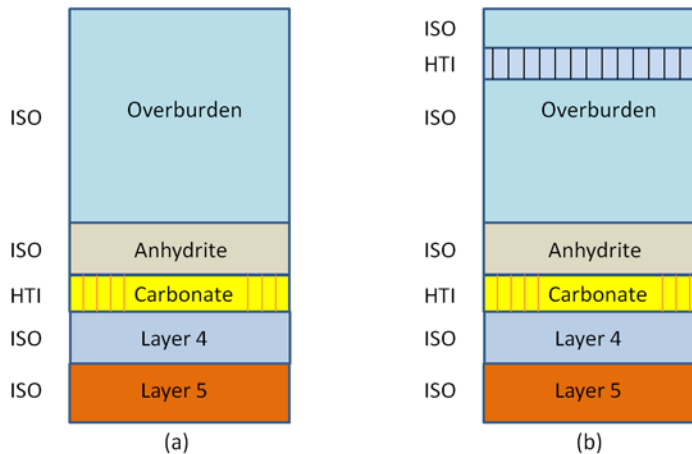
Figure 3. (a) Forward model including anhydrite cap rock and vertically fractured carbonate reservoir and isotropic overburden. (b) Same model with added anisotropic section in the overburden.
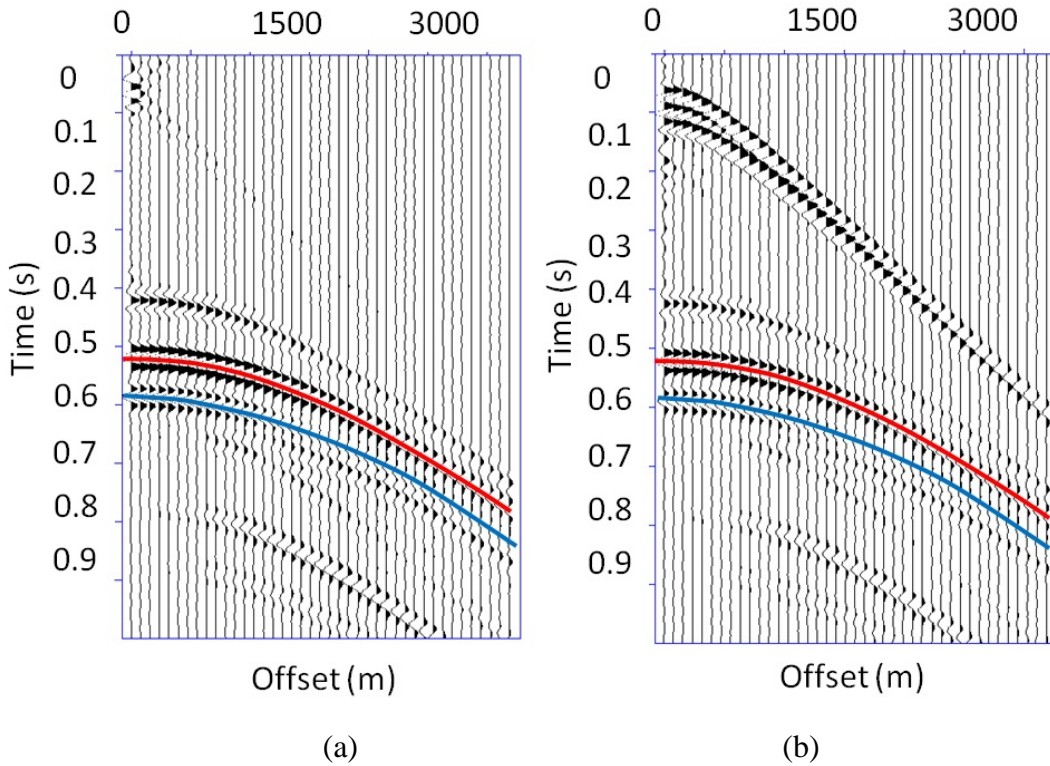
Figure 4. Full-waveform synthetic CDP gathers for two models. One with isotropic overburden (a) and the other is with anisotropic overburden (b). Red and blue picks denote reservoir top and a reflector below reservoir respectively.

CONVENTIONAL AVOA ANALYSIS

Reflection amplitudes for both reservoir top (Anhydrite/Reservoir interface) and for a reflector below the reservoir (Layer 4/Layer 5 in figure 3) are picked for all source-receiver azimuths. Bottom of reservoir reflection (Reservoir/Layer 4) is not evident in the synthetic gathers because of the smooth transition in rock properties between the two layers. Figure 5 shows the AVOA curves for reservoir top (a) and for a reflector below the reservoir (b) at different azimuths for the model with isotropic overburden. The 0 and 90 degree azimuths correspond to a seismic wave traveling across and along fractures, respectively. Earth is complicated in nature and the assumption of isotropic overburden is not usually valid. Figure 6 shows the AVOA response of both reservoir top (a) and for a reflector below the reservoir (b) which represents model (b) in figure 3. Here the overburden has one anisotropic layer caused by one set of vertical fractures. Zero degree azimuth corresponds to a seismic wave traveling across fractures in the reservoir section and along fractures in the anisotropic layer in the overburden. Figure 6 shows that the AVOA response has been greatly affected by the existence of the anisotropic overburden, which could cause erroneous estimation of reservoir fracture parameters.

PROPOSED METHOD

Seismic gathers for two models - one with isotropic overburden (Figure 4a) and the other with anisotropic overburden (Figure 4b) are transformed to the delay-time slowness (tau-p) domain (Figure 7 a, b). The red and blue lines correspond to reservoir top and a reflector below reservoir respectively. The ratio of amplitudes from both reflectors is taken in order to remove transmission effect from the overburden. The ratio equation is:

$$Ratio = \frac{T_{1\to2}^{down} T_{2\to3}^{down} R_3 T_{3\to2}^{up} T_{2\to1}^{up}}{T_{1\to2}^{down} R_2 T_{2\to1}^{up}} = T_{2\to3}^{down} \left(\frac{R_3}{R_2}\right) T_{3\to2}^{up} \ , \tag{1}$$

where $T_{1\to2}^{down}, T_{2\to1}^{up}, T_{2\to3}^{down}, T_{3\to2}^{up}$ are upward and downward transmission amplitudes between layers 1, 2 and 3. $R_2 \ and \ R_3$ are reflection amplitudes for layer interface. Figure 8 shows the model used for equation 1.

The ratio results for the two models can be seen in figure 9 a, b. The overburden effect, which hindered AVOA analysis is greatly reduced and the ratio attributes in both are almost identical. Fracture parameters can now correctly be estimated.

If the ratio of the two horizons is taken in the t-x domain, overburden effect is not removed as shown in figure 10 a, b. This indicates that the tau-p is the correct domain to take the ratio attribute, where each trace in figure 7 has one ray parameter value.

INVERSION OF NORMAL AND TANGENTIAL WEAKNESSES

In this part of the paper we quantitatively analyze reservoir fracture properties, namely, fracture normal and tangential weaknesses or ΔN and ΔT respectively. The inversion is performed on synthetic CDP gathers generated in the previous section. The first step is to do a conventional inversion using AVOA data and see which parameter is reliable. The second step is to apply the inversion to the ratio attribute where overburden effect is believed to be removed.

Theory

Reflection of HTI medium causes amplitude variation with offset and azimuth (AVOA) and been studied extensively (Mallick and Frazer, 1991; Rüger, 1998; Rüger and Tsvankin, 1997, Alhussain et al., 2007). Thomsen's (1986) weak anisotropy parameters for HTI medium
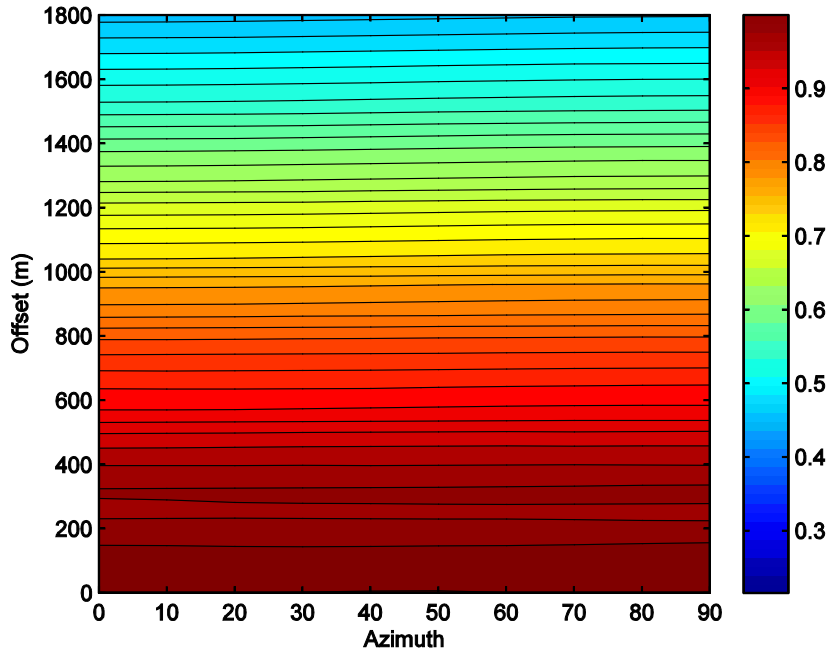
(a)
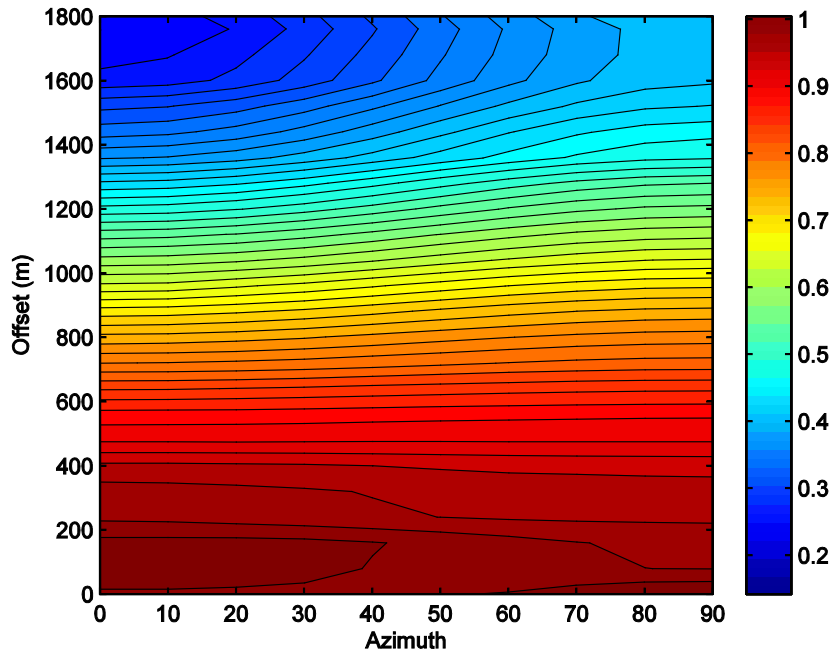
(b)

Figure 5. AVOA response of reservoir top (a) and for a reflector below the reservoir (b) for a model which has isotropic overburden.

Estimation of fracture parameters

(a)

(b)
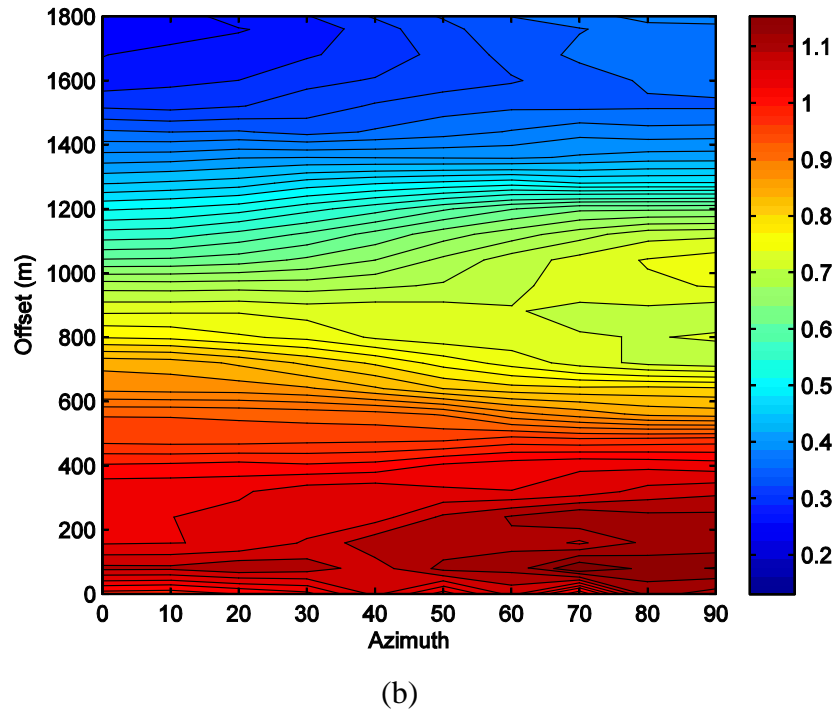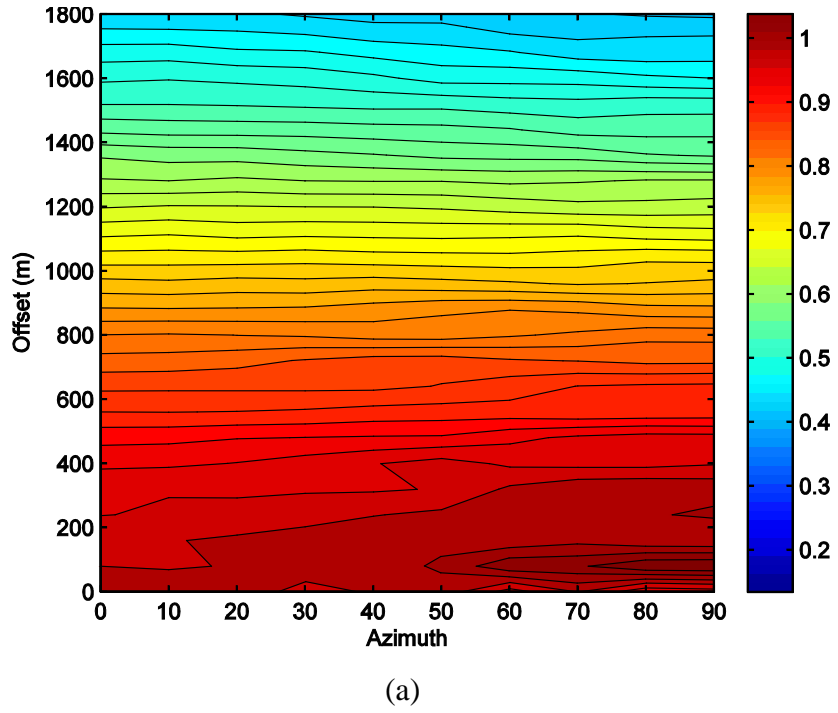
Figure 6. AVOA response of reservoir top (a) and for a reflector below the reservoir (b) for a model which has anisotropic overburden.
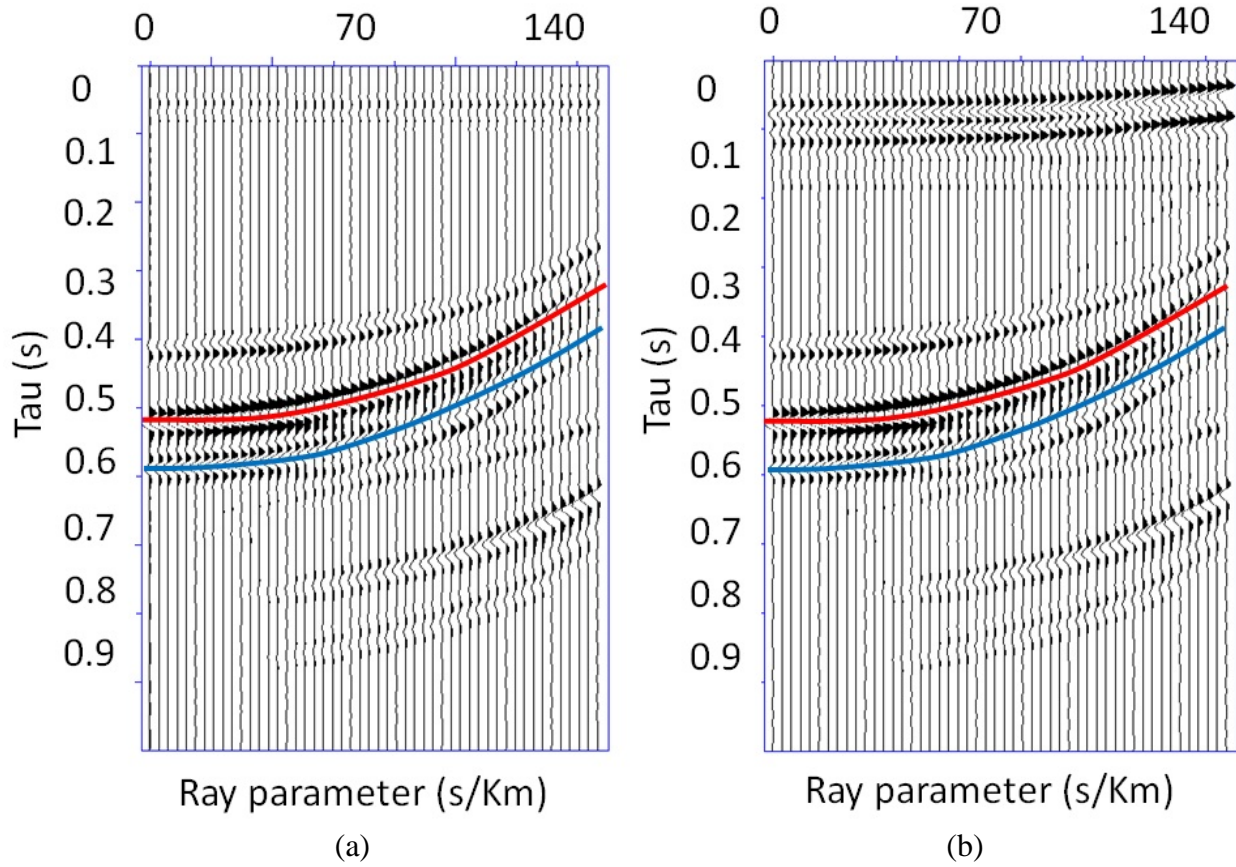
Figure 7. Transformed CDP gathers in the tau-p domain for both the model with isotropic overburden (a) and anisotropic overburden (b). The red and blue lines correspond to reservoir top and a reflector below reservoir picks respectively.
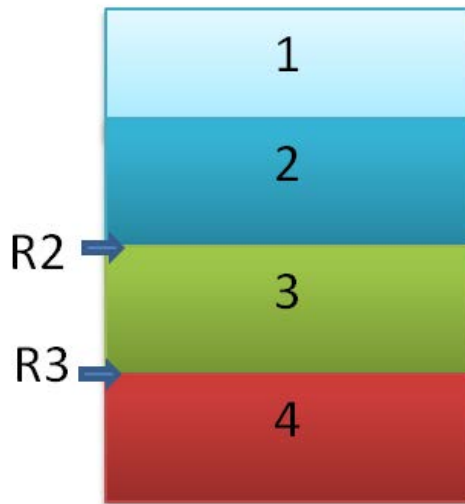
Figure 8. A four layers model where R2 and R3 are defined in equation 1.
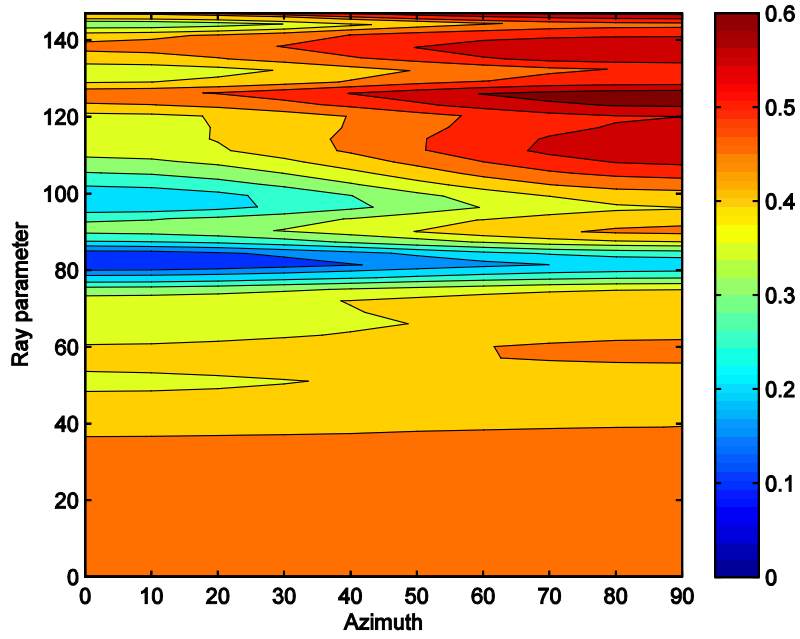
(a)
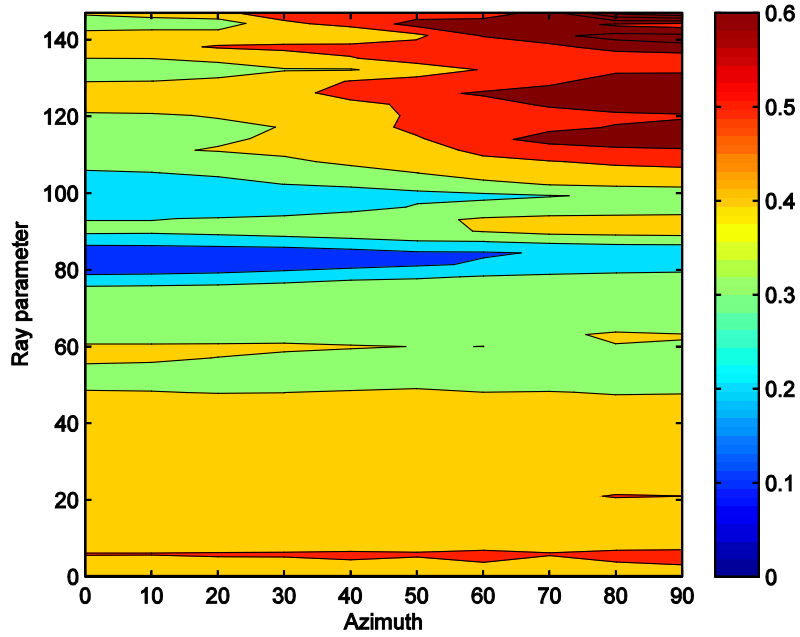
(b)

Figure 9. Ratio for reservoir top and a reflector below reservoir picks in the tau-p domain for two models one with isotropic overburden (a) and the other with anisotropic overburden (b).

(a)

(b)
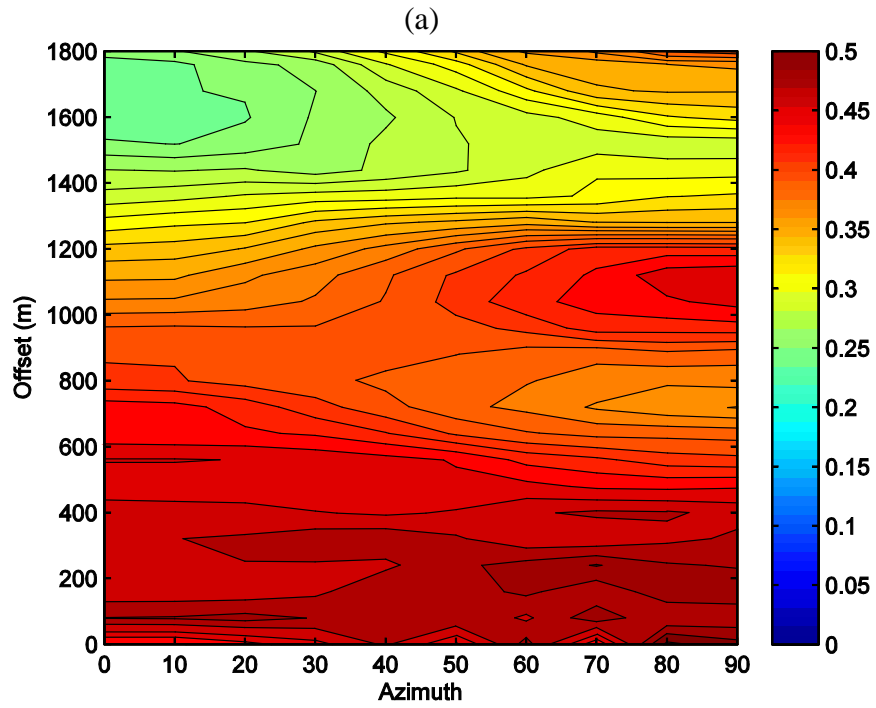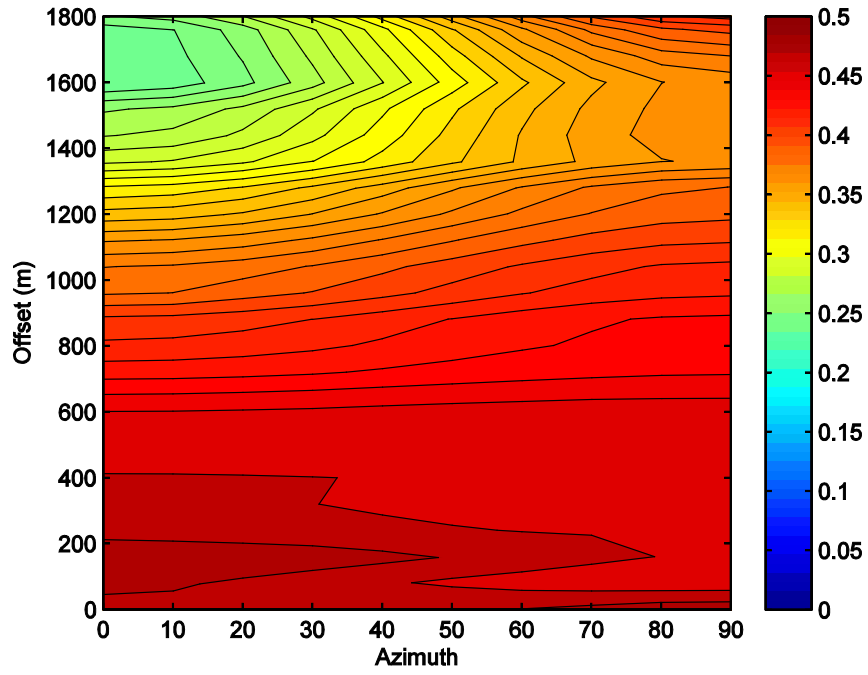
Figure 10. Ratio for reservoir top and a reflector below reservoir picks in the t-x domain for two models one with isotropic overburden (a) and the other with anisotropic overburden (b).

$(\epsilon^{v}, \delta^{v}, \gamma^{v})$ are used routinely to represent TI media and have a simple relationship to stiffness coefficients (Bakulin et al., 2000):

$$\epsilon^{(v)} = \frac{C_{11} - C_{33}}{2C_{33}}, \tag{2}$$

$$\delta^{(v)} = \frac{(C_{13} + C_{55})^2 - (C_{13} - C_{55})^2}{2C_{33}(C_{33} - C_{55})}, \tag{3}$$

$$\gamma^{(v)} = \frac{C_{66} - C_{44}}{2C_{44}}. \tag{4}$$

Fracture weaknesses can be computed directly from both Thomson's parameters and Vp/Vs ratio (Bakulin et al., 2000):

$$\Delta N = -\frac{\epsilon^{(v)}}{2g(1-g)}, \tag{5}$$

$$\Delta T = \frac{1}{2g}\left[\frac{1-2g}{1-g}\epsilon^{(v)} - \delta^{(v)}\right], \tag{6}$$

$$g = \frac{V_s^2}{V_p^2}. \tag{7}$$

Shaw and Sen (2006) expressed AVOA reflection coefficients directly as a function of fracture weaknesses as follows:

$$R^{total}(\theta, \emptyset) = R^{iso}(\theta) + R^{ani}(\theta, \emptyset, \Delta), \tag{8}$$

$$\Delta^T = (\Delta N, \Delta V, \Delta H, \Delta NV, \Delta NH, \Delta VH). \tag{9}$$

R^{iso} represents the isotropic part of reflection coefficient and depends only on reflection angle θ. R^{ani} is the anisotropic part of reflection coefficient and is a function of reflection angle θ, azimuth $\emptyset$, and fracture weaknesses Δ. Shaw and Sen (2004) linearized reflection coefficients by presenting a weak anisotropic medium as a volume of scatterers embedded in a background isotropic medium. They used asymptotic ray theory and the method of stationary phase to show that the scattering function $S(r_0)$ corresponding to the singly scattered wavefield relates to the linearized PP-reflection coefficients as:

$$R_{pp}(\theta) = \frac{1}{4\rho_0 \cos^2(\theta)} S(r_0), \tag{10}$$

$$S(r_0) = \Delta\rho\xi + \Delta_{C_{ijkl}}\eta_{ijkl}, \tag{11}$$

$$\xi = t_i t_j'|_{r=r_0}, \tag{12}$$

$$\eta_{ijkl} = t_i' p_j' t_k p_l|_{r=r_0}, \tag{13}$$

where ρ_0 is the density of the background medium. $\Delta\rho$ is perturbation in density and $\Delta_{C_{ijkl}}$ is perturbation in the elastic stiffness. p is the slowness and t is the polarization vectors. The scattered wave is denoted by a prime. The position vector r_0 is the point on a horizontal interface which separates two weak isotropic or anisotropic media.

Shaw and Sen (2006) derived the dependence of PP-reflection coefficients on fracture weaknesses by collecting the coefficients η_{ijkl} corresponding to each weakness. Under the assumption of small fracture weakness the derived equation is:

$$\delta R = R_{pp}^{obs}(\theta, \emptyset) - R_{pp}^{iso}(\theta) = A\Delta, \tag{14}$$

$$A = \frac{1}{4}[a_N, a_V, a_H, a_{NV}, a_{NH}, a_{VH}], \tag{15}$$

were R_{pp}^{obs} is the observed reflection coefficient and R_{pp}^{iso} is the reflection coefficient of the isotopic background. A is the sensitivity matrix. For a given incidence angle and azimuth, the row elements of A are given by:

$$a_N = (1 - 2g)^2 + [(1 - 2g) + 2g(1 - 2g)cos2\emptyset]sin^2\theta + \left[\left(1 - 2g + \frac{3}{2}g^2\right) + 2g(1 - g)cos2\emptyset + \frac{1}{2}g^2cos4\emptyset\right]sin^2\theta tan^2\theta, \tag{16}$$

$$a_v = -2g(1 + cos2\emptyset)sin^2\theta, \tag{17}$$

$$a_H = \frac{g}{2}(1 - cos4\emptyset)sin^2\theta tan^2\theta, \tag{18}$$

$$a_{NV} = 0, \tag{19}$$

$$a_{NH} = 2\sqrt{g}(1 - g)sin2\emptyset sin^2\theta + \sqrt{g}[2(1 - g)sing2\emptyset + gsing4\emptyset]sin^2\theta tan^2\theta, \tag{20}$$

$$a_{VH} = 0. \tag{21}$$

Estimation of ΔN and ΔT from fractured synthetic models

The synthetic model introduced in the previous section is used here to invert for ΔN and ΔT. The model consists of a vertically fractured reservoir which is divided into 14 compartments (Figure 2) representing the gradual change in vp, vs, density and porosity within the reservoir. The reservoir has an isotropic overburden layer on top. The AVOA response of the reflector

below the reservoir is used to invert for ΔN and ΔT parameters. ΔN and ΔT for each reservoir compartment are calculated directly from elastic coefficients of HTI medium using equations 2, 3, 5 and 6. Elastic coefficients that are used as an input to the numerical simulation and correspondent ΔN and ΔT values are shown in table 1. Both parameters are almost constant in all reservoir units and the average values are 0.62 and 0.14 for ΔN and ΔT respectively. This is extremely helpful because we are inverting for one value for each parameter that represents the entire reservoir unit.

Table 1. HTI elastic stiffness parameters for 14 reservoir compartments and the computed normal (ΔN) and tangential (ΔT) weakness parameters.

Compartment	C11	C33	C13	C44	C55	ΔN	ΔT
1	15.2	31.2	6.8	10.1	7.8	0.58	0.14
2	16.5	33.7	7.6	10.7	8.3	0.58	0.14
3	17.7	36.6	7.9	11.7	9.1	0.59	0.14
4	18.6	38.9	8.4	12.4	9.6	0.60	0.14
5	20.1	42.2	8.6	13.8	10.7	0.60	0.14
6	21.8	46.7	9.7	14.9	11.6	0.62	0.14
7	23.6	49.6	9.8	16.4	12.7	0.60	0.15
8	25.4	52.7	10.9	17.2	13.3	0.59	0.15
9	27.9	58.7	11.6	19.4	15.0	0.60	0.15
10	27.2	59.1	12.3	18.8	14.6	0.65	0.14
11	28.3	61.9	12.9	19.5	15.2	0.65	0.14
12	31.6	68.7	13.7	22.2	17.2	0.64	0.14
13	33.3	70.2	14.9	22.4	17.5	0.63	0.14
14	36.2	75.2	16.1	23.8	18.5	0.62	0.14

AVOA inversion of ΔN and ΔT parameters

Equation 14 is used to invert for ΔN and ΔT parameters. In order to perform the inversion, knowledge of the orientation of the vertical fractures as well as information about the physical parameters of isotropic background (Vp/Vs) are required. For the synthetic example, both parameters are available. In equation 14 the term $R_{pp}^{iso}(\theta)$ is the reflection coefficient for the interface separating the overlying medium from the isotropic medium in which fractures are embedded. $R_{pp}^{iso}(\theta)$ is set to be equal to $R_{pp}^{fracture\,parallel}(\theta)$ where seismic waves do not see factures as they travel parallel to them. The isotropic reflection coefficient term is subtracted from the observed amplitude data to isolate the effect of fractures on the AVOA.

A linear least-squares inversion is performed to estimate the fracture weaknesses ΔN and ΔT:

$$\Delta = [A^T A]^{-1} A^T \delta R, \tag{22}$$

where $\Delta^T = [\Delta N \; \Delta T]$ and we set $a^T = (a^V + a^H)/2$.

Inverted ΔN and ΔT are equal to 0.64 and -0.048 respectively and the average values calculated directly from input parameters are 0.62 and 0.14. This means that ΔN is successfully inverted for but ΔT is not. I attribute this difficulty in the parameter estimation to the complexity of equations 3 and 6 where ΔT depends on many medium parameters for accurate prediction. It depends on $C_{11}, C_{33}, C_{13}, C_{55}, and \; v_p/v_s$. The effect of ΔT on PP-reflection coefficients is prominent at large angles of incidence only (Shaw and Sen, 2006). This behavior is similar to the effect of S-wave velocity on PP-reflection coefficient from an interface separating two isotropic media. On the other hand, ΔN depend only on $C_{11}, C_{33}, and \; v_p/v_s$ and the effect of ΔN on the reflection coefficients is at most incidence angles.

It is important to understand the significance of ΔN and how it is related to fracture parameter prediction. Note that ΔN is directly related to crack density by the following relation:

$$\Delta N = \frac{4e}{3g(1-g)},$$ (23)

where e is crack density and $g = \frac{V_s^2}{V_p^2}$.

Assuming that we have an accurate value Vp/Vs ratio we can have a good idea about crack density and ΔN can be used to estimate the fracture density parameter.

Proposed ΔN and ΔT inversion method

In the first part of this paper a method to remove the effect of an anisotropic overburden in order to recover true reservoir fracture parameters is presented. It involves analyzing AVOA for a reservoir pick and for a reflector below the reservoir. Seismic gathers are transformed to delay-time slowness domain and the ratio of reservoir pick to the reflector below the reservoir is taken in order to remove transmission effect from the overburden. The ratio attribute which corresponds to two models one has an isotropic overburden (Figure 3a) and the other has anisotropic overburden (Figure 3b) are used here to invert for both ΔN and ΔT parameters. Equation 14 is modified in order to use ratio amplitudes instead of conventional AVOA as follows:

$$\delta R = Rratio_{pp}^{obs}(\theta, \emptyset) - Rratio_{pp}^{iso}(\theta) = \frac{A}{R_{pp}^{top}(\theta,\emptyset)*\propto}\Delta,$$ (24)

where $Rratio_{pp}^{obs}$ is amplitudes for observed data and is a function of angle and azimuth. $Rratio_{pp}^{iso}$ is the amplitude for the isotropic background and is a function of angles. A is the sensitivity matrix defined in equations 16 to 21 which is normalized by R_{pp}^{top}. $\propto$ is a scalar.

Inversion results of both models (Isotropic and anisotropic overburden) are 0.551 and 0.546 for ΔN and -5.94 and -8.6 respectively. It can be concluded that ΔN is reasonably estimated (%11 and %12 error) when compared to derived value (0.62) from HTI elastic coefficients. I believe this discrepancy in ΔN is related to the composite effect of the term: $T_{2 \to 3}^{down}(R_3/R_2)T_{3 \to 2}^{up}$ of equation 1. The ratio of reflection coefficient of a reflector below the reservoir R_3 and reservoir top R_2 at different angles of incidence and azimuth could be the cause of the deviation of ΔN estimation. Overall, the ΔN parameter can be successfully inverted for using the ratio method. On the other hand, the inversion of ΔT parameters is unstable for the same reasons mentioned in the previous section.

CONCLUSIONS

We presented a method to remove the effect of an anisotropic overburden in order to recover true reservoir fracture parameters. It involves analyzing AVOA for a reservoir pick and for a reflector below the reservoir. Seismic gathers are transformed to delay-time slowness (tau-px,py or tau-p,azimuth) domain and the ratio of reservoir pick to the layer below the reservoir is taken in order to remove transmission effect from the overburden. Note that it is the ray-parameter and not the angle that remains constant in different layers and that the reflection/transmission coefficients are fundamentally functions of ray-parameters. That is precisely the reason as to why the ratio method works better in tau-p than in x-t domain. The method is applied to two sets of forward models one containing fractured reservoir with isotropic overburden and the other is the same model but with anisotropic overburden. Conventional analysis in the t-x domain shows that the anisotropic overburden has completely obscured the anisotropic estimation. When the new method is applied, the overburden effect was removed and more reliable anisotropic fracture parameter estimation can be reached.

Conventional AVOA inversion results applied to a synthetic model shows that ΔN parameter is reliably inverted for as long as the background isotropic parameter is estimated with good accuracy. This information is usually taken from well logs. On the other hand, inversion for ΔT parameter from Rpp azimuthal response is not successful and I attribute that to the dependence of ΔT on many medium parameters for accurate prediction. It depends on $C_{11}, C_{33}, C_{13}, C_{55},$ and v_p/v_s. Another reason is that effect of ΔT on PP-reflection coefficients is prominent at large angles of incidence only.

The inversion is also applied to the ratio attribute where overburden effect is believed to have been removed. ΔN is also reliably inverted for with some discrepancy (11% and 12% errors) which I believe is related to the composite effect of the term: $T_{2\to3}^{down}(R_3/R_2)T_{3\to2}^{up}$ of equation 1. The ratio of reflection coefficient of a reflector below the reservoir R_3 and reservoir top R_2 at different angle of incidence and azimuth could be the cause of the deviation of ΔN estimation. It is important to note that the ΔN parameter is directly proportional to fracture density (equation 23) and high ΔN values can be attributed to high crack density values.

ACKNOWLEDGEMENT

APPENDIX A

Linear-slip theory

The starting point of the derivation is the fundamental idea of linear-slip theory (Schoenberg and Sayers, 1995) which states that fractures can be represented as either infinitely thin and high compliant layers or planes of weakness with linear-slip or non-welded boundary conditions (Bakulin et al., 2000). The displacement discontinuity (u) is assumed to be linearly related to the stress traction (σ) which is continuous across the interface (Schoenberg, 1980). The equations describing displacement and stress across an interface are:

$$[\sigma_{11}] = [\sigma_{12}] = [\sigma_{13}] = 0, \tag{A1}$$

$$[u_1] = h(K_N\sigma_{11} + K_{NH}\sigma_{12} + K_{NV}\sigma_{13}), \tag{A2}$$

$$[u_2] = h(K_{NH}\sigma_{11} + K_H\sigma_{12} + K_{VH}\sigma_{13)}, \tag{A3}$$

$$[u_3] = h(K_{NV}\sigma_{11} + K_{VH}\sigma_{12} + K_V\sigma_{13}). \tag{A4}$$

where h is the average distance between the fractures and the brackets denote the jump of the values across the interface.

A medium that is homogeneous and isotropic and embedded with a set of parallel vertical fractures can be represented by liner slip model and the effective stiffness matrix is derived by Schoenberg and Sayers (1995):

$$C = (\lambda + 2\mu)[C^b - C^f], \tag{A5}$$

$$C^b = \begin{bmatrix} 1 & x & x & 0 & 0 & 0 \\ & 1 & x & 0 & 0 & 0 \\ & & 1 & 0 & 0 & 0 \\ & & & g & 0 & 0 \\ & & & & g & 0 \\ & & & & & g \end{bmatrix}, \tag{A6}$$

$$C^f = \begin{bmatrix} \Delta N & x\Delta N & x\Delta N & 0 & \sqrt{g}\Delta NV & \sqrt{g}\Delta NH \\ & x^2\Delta N & x^2\Delta N & 0 & x\sqrt{g}\Delta NV & x\sqrt{g}\Delta NH \\ & & & 0 & x\sqrt{g}\Delta NV & x\sqrt{g}\Delta NH \\ & & & 0 & 0 & 0 \\ & & & & g\Delta V & g\sqrt{g}\Delta VH \\ & & & & & g\Delta H \end{bmatrix}. \tag{A7}$$

where λ and μ are Lame's parameters, $g = \frac{\mu}{\lambda+2\mu} = \frac{V_s^2}{V_p^2}$. $x = \frac{\lambda}{\lambda+2\mu} = 1 - 2g$, and the fracture weaknesses are defined by:

$$\Delta N = \frac{(\lambda+2\mu)K_N}{1+(\lambda+2\mu)K_N}, \tag{A8}$$

$$\Delta NV = \frac{\sqrt{\mu(\lambda+2\mu)}K_{NV}}{1+\sqrt{\mu(\lambda+2\mu)}K_{NV}}, \tag{A9}$$

$$\Delta V = \frac{\mu K_V}{1+\mu K_V}, \tag{A10}$$

$$\Delta NH = \frac{\sqrt{\mu(\lambda+2\mu)}K_{NH}}{1+\sqrt{\mu(\lambda+2\mu)}K_{NH}}, \tag{A11}$$

$$\Delta H = \frac{\mu K_H}{1+\mu K_H}, \tag{A12}$$

$$\Delta VH = \frac{\sqrt{\mu(\lambda+2\mu)}K_{VH}}{1+\sqrt{\mu(\lambda+2\mu)}K_{VH}}. \tag{A13}$$

The fracture stiffness matrix in equation (6.7) corresponds to a medium with monoclinic symmetry. Two assumptions are made in order to reduce the symmetry to horizontal transverse isotropic (HTI) medium:

1. Fractures are invariant under rotation about the normal to the facture faces (rotationally invariant)
2. Fractures have no corrugation or surface roughness

The above assumptions result in:

$$K_{NV} = K_{NH} = K_{VH} = 0, \Delta NV = \Delta NH = \Delta VH = 0, \text{ and}$$

$$K_V = K_H = K_T, \ \Delta V = \Delta H = \Delta T. \tag{A14}$$

Appendix B

Poroelatic fractured model (Gurevich, 2003)

Explicit analytical expressions are derived for the low-frequency elastic constants and anisotropy parameters of a fractured porous medium saturated with a given fluid (Figure B1). The five elastic constants of the resultant transversely isotropic (TI) medium are derived as a function of the properties of the dry (isotropic) background porous matrix, fracture properties and fluid bulk modulus. The derivation is based on a combination of the anisotropic form of Gassmann (1951) equation and the liner-slip model (explained in appendix A). The elastic constants of the fluid-saturated media are:

$$C_{11}^{sat} = \frac{L}{D} \left\{ d_1 \theta + \frac{K_f}{\phi K_g L} \left[L_1 \alpha' - \frac{16}{9} \frac{\mu^2 \alpha_0}{L} \Delta_N \right] \right\}, \tag{B1}$$

$$C_{33}^{sat} = \frac{L}{D} \left\{ d_2 \theta + \frac{K_f}{\phi K_g L} \left[L_1 \alpha' - \frac{4}{9} \frac{\mu^2 \alpha_0}{L} \Delta_N \right] \right\}, \tag{B2}$$

$$C_{13}^{sat} = \frac{L}{D} \left\{ d_2 \theta + \frac{K_f}{\phi K_g L} \left[L_1 \alpha' - \frac{4}{9} \frac{\mu^2 \alpha_0}{L} \Delta_N \right] \right\}, \tag{B3}$$

$$C_{44}^{sat} = \mu, \tag{B4}$$

$$C_{55}^{sat} = \mu(1 - \Delta_T), \tag{B5}$$

where

$$D = 1 + \frac{K_f}{K_g \phi}(\alpha_0 - \phi + \frac{K^2 \Delta_N}{K_g L}), \qquad \theta = 1 - \frac{K_f}{K_g}, \alpha' = \alpha_0 + \frac{K^2}{K_g L} \Delta_N,$$

$$K = \lambda + \frac{2\mu}{3}, L = \lambda + 2\mu, \alpha_0 = 1 - \frac{K}{K_g}.$$

The parameter ϕ is the overall porosity of the porous fractured rock (sum of background porosity and fracture prosoity). K_g and K_f are bulk modulus of grain and fluid respectively. ΔN and ΔT are dimensionless fracture weakness.
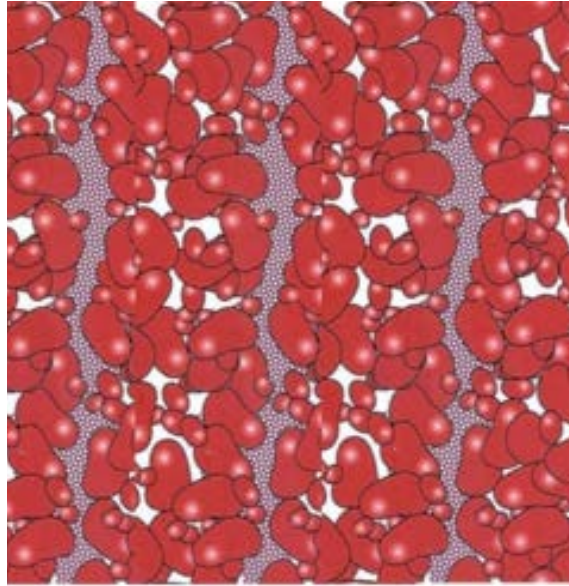
Figure B1. Schematic of porous fractured reservoir. The white color is the Vogt space and the blue color represents vertical factures. Both Vogt space and fractures are filled with a fluid (after Gurevich, 2009).

REFERENCES

Alhussain, M. A., 2007, AVOaz response of a fractured medium: Laboratory measurements versus numerical simulations, 78th Annual International Meeting, SEG, Expanded Abstracts, 1-4.

Bakulin, A., I. Tsvankin, and V. Grechka, 2000, Estimation of fracture parameters from reflection seismic data-Part I: HTI model due to a single fracture set: Geophysics, **65**, 1788-1802.

Gassmann, F., 1951, Elastic waves through a packing of sphere: Geophysics, **16**, 673-685.

Gurevich, B., 2003, Elastic properties of saturated porous rocks with aligned fractures: Journal of Applied Geophysics, **54**, 203-218.

Gurevich, B., M. Brajanovski, R. J. Galvin, T. M. Muller, and J. Toms-Stewant, 2009, P-wave dispersion and attenuation in fractured and porous reservoirs – poroelasticity approach, Geophysical Prospecting, **57**, 225-237.

Liu, E., G. Zelewski, C. Lu, J. M. Reilly and Z. J. Shevchek, 2011, Mitigation of overburden effects in fracture prediction using azimuthal AVO analysis: The Leading Edge, **30**, 750-756.

Luo, M., I. Takahashi, M. Takanashi, and Y. Tamura, 2005, Improved fracture network mapping through reducing overburden influence: The Leading Edge, **24**, 1094-1098.

Luo, M., M. Takanashi, K. Nakayama, and T. Ezaka, 2007, Physical modeling of overburden effects: Geophysics, **72**, T37-T45.

Mallick, S., and L. N. Frazer, 1991, Reflection/transmission coefficients and azimuthal anisotropy in marine seismic studies: Geophysical Journal International, **105**, 241-252.

Rüger, A., 1998, Variation of P-wave reflectivity with offset and azimuth in anisotropic media: Geophysics, **63**, 935-947.

Rüger, A., I. Tsvankin, 1997, Using AVO for fracture detection: Analytic basis and practical solutions: The Leading Edge, **16**, 1429-1434.

Sayers, C., and J. E. Rickett, 1997, Azimuthal variation of AVO response for fractured gas sands: Geophysical Prospecting, **45**, 187-192.

Schoenberg, M., 1980, Elastic wave behavior across linear slip interfaces: Journal of the Acoustical Society of America, **68**, 1516-1521.

Schoenberg, M., and C. Sayers, 1995, Seismic anisotropy of fractured rock: Geophysics, **60**, 204-211.

Schoenberg, M., J. Douma, 1988, Elastic wave propagation in media with parallel fractures and aligned cracks: Geophysical Prospecting, **36**, 571-590.

Sen, M. K., 2007, Anomalous reflection amplitudes from fractured reservoirs – Failure or AVOA?: The Leading Edge, **26**, 1148-1152.

Shaw, R. K., and M. K. Sen, 2004, Born integral, stationary phase and linearized reflection coefficients in weak anisotropic media, Geophysical Journal International, **158**, 225-238.

Shaw, R. K., and M. K. Sen, 2006, Use of AVOA data to estimate fluid indicator in a vertically fractured medium, Geophysics, **71(3)**, C15-C24.

Thomsen, L., 1986, Weak elastic anisotropy: Geophysics, **51**, 1954-1966.

Tsvankin, I., 2005 Seismic signatures and analysis of reflection data in anisotropic media: *Elsevier Science*, second edition.